Adsorption and Dehydrogenation of *Ortho*-Carborane on the Pt(111) Surface

Aashani Tillekaratne, David Siap,[†] and Michael Trenary*

Department of Chemistry, University of Illinois at Chicago, 845 W. Taylor Street, Chicago, Illinois 60607-7061

Received: February 9, 2008; Revised Manuscript Received: February 29, 2008

The surface chemistry of 1,2-*closo*-dicarbadodecaborane (*ortho*-carborane), $C_2B_{10}H_{12}$, on Pt(111), was studied with reflection–absorption infrared spectroscopy (RAIRS), temperature programmed desorption, and X-ray photoelectron spectroscopy (XPS). This molecule has a cage-like structure in which boron and carbon atoms occupy the vertices of a slightly distorted icosahedron with 2 C−H and 10 B−H radially directed bonds. At submonolayer coverages at 85 K, the RAIRS spectrum of carborane displays strong B−H stretching vibrations near 2600 cm^{-1} and a weak C−H stretch at 3090 cm^{-1} that are close in value to those of the isolated molecule. This indicates molecular adsorption at low temperature. At 85 K and low coverages, the B−H stretch peaks of carborane are unusually narrow with full widths at half-maxima as low as 4.4 cm^{-1}. Comparison of calculated spectra for various assumed orientations reveals that the molecule is oriented with its permanent dipole moment and the C−C bond parallel to the surface. The molecule is stable on the surface up to 250 K, where it is transformed into a new intermediate with a strongly red-shifted B−H stretch vibration at 2507 cm^{-1}. This intermediate is stable up to 400 K, above which no B−H stretch vibrations are observed. Hydrogen is released in stages as the carborane monolayer is heated from 85 to 800 K, indicating the formation of partially hydrogenated surface intermediates. From XPS measurements of the B 1s peak area as a function of annealing temperature, the boron coverage steadily decreases as the boron cage structure is disrupted and boron atoms diffuse into the bulk of the crystal.

Introduction

Boranes and carboranes constitute a unique and interesting class of molecules that feature three-dimensional cage structures and an extensive use of three-center two-electron bonds.[1–8] Furthermore, a long-active area of research[1,2,8–15] has been the interaction of boranes and carboranes with metals to form metalloboranes and metallocarboranes. Classic examples of the latter are metal complexes with the dicarbollide anion, $C_2B_9H_{11}^{2-}$, that is obtained from the icosahedral 1,2-dicarbadodecaborane, $C_2B_{10}H_{12}$, by removing one BH bond from a vertex thus exposing a five-membered C_2B_3 ring that bonds to metals in a fashion similar to that of the cyclopentadienyl ($C_5H_5^-$) anion. Thus, the dicarbollide analogues of ferrocene and related complexes are well-known. Although the interaction of boranes and carboranes with metals to form metalloboranes and metallocarboranes has been extensively studied, with only a few exceptions,[16–24] little is known about their interaction with metal surfaces. However, an understanding of such interactions is important for both fundamental as well as applied objectives. For example, carborane is a precursor gas for the growth of boron carbide thin films by chemical vapor deposition (CVD).[16–20] Also, for hydrogen storage applications, transition metal catalysts are being studied as promoters of low temperature release of hydrogen from complex hydrides,[25] many of which include boron compounds.

Vibrational spectroscopy can be a powerful tool for determining if and how the structure of a molecule changes upon adsorption onto a surface. The structure of the molecule studied here, *closo*-1,2-dicarbadodecaborane, which is commonly referred to as *ortho*-carborane and is the most common of the three isomers of $C_2B_{10}H_{12}$, is shown in Figure 1. The other isomers are *closo*-1,7-dicarbadodecaborane (*meta*-carborane) and *closo*-1,12-dicarbadodecaborane (*para*-carborane). Although *ortho*-carborane has C_{2v} symmetry, it is closely related to the much more symmetric *closo*-dodecaborate anion, $B_{12}H_{12}^{2-}$, which has the structure of a regular icosahedron, by replacing two BH^- units with two CH units. Both molecules have 24 atoms and hence 66 normal modes of vibration. Because of its icosahedral symmetry, $B_{12}H_{12}^{2-}$ has only one IR active irreducible representation, T_{1u}, which gives rise to three fundamentals in the IR spectrum, the strongest of which is due to a B−H stretch mode at 2485 cm^{-1}.[26] In the reduced symmetry of $C_2B_{10}H_{12}$, the

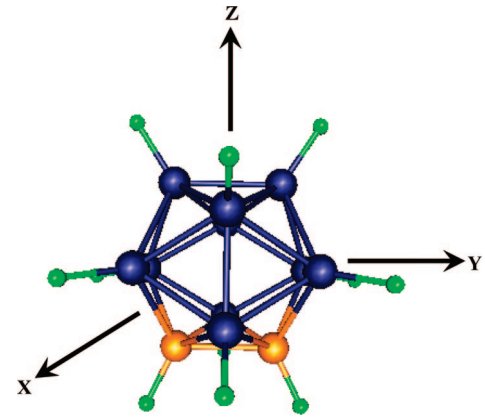

Figure 1. Structure of *ortho*-carborane (1,2-*closo*-dicarbadodecaborane), $C_2B_{10}H_{12}$. Boron atoms are shown in blue; carbon atoms are in orange, and the hydrogen atoms are in green. It has a slightly distorted icosahedral structure and belongs to the C_{2v} point group. The *z* axis is defined to be along the 2-fold rotation axis; the *y* axis is defined to be parallel to the C−C bond, and the *x* axis is defined to be perpendicular to the C−C bond.

* Corresponding author. E-mail: mtrenary@uic.edu.
[†] Present address: Department of Mathematics, University of Illinois, Urbana–Champaign, IL 61801.

10.1021/jp8011975 CCC: $40.75
Published on Web 05/14/2008

normal modes are assigned to the irreducible representations of the C_{2v} point group as follows:

$$\Gamma_{vib} = 21A_1 + 13A_2 + 16B_1 + 16B_2$$

Since only the A_2 modes are IR inactive, 53 IR active fundamentals are formally allowed by symmetry. However, the distortion of $C_2B_{10}H_{12}$ from icosahedral symmetry is slight; the spectra are not much different from that of $B_{12}H_{12}^{2-}$, and relatively few of the allowed modes have appreciable IR intensity. This experimental observation is in accord with the Hartree–Fock and density functional theory calculations reported by Salam et al.[27]

The present study is designed to address several issues in the surface chemistry of carborane on Pt(111). Does it adsorb molecularly or dissociatively, and if it is the former, does it do so with a preferred orientation? Can the Pt surface promote the dissociation of the B−H and C−H bonds so that the molecule dehydrogenates at a much lower temperature than its bulk decomposition temperature? Most importantly, are stable surface intermediates formed in the course of its thermal decomposition? Since carborane is used as a precursor gas to produce thin films of boron carbide, which has a structure containing $B_{11}C$ icosahedral units, a key question is whether the icosahedral cage structure is retained in any stable surface intermediates that may form. Some of these issues have been explored in previous studies. For example, Zeng et al.[23] found that carborane adsorbs molecularly on Cu(100) at temperatures below 180 K but dissociatively at 300 K.

Experimental Section

The experiments were performed in two different ultra high vacuum (UHV) chambers using two different Pt(111) single crystals. The X-ray photoelectron spectra were obtained in a chamber (chamber 1) with a base pressure of $\sim 1 \times 10^{-10}$ Torr. The system has been described in detail elsewhere.[28] In brief, the UHV chamber is equipped with low energy electron diffraction (LEED), an X-ray photoelectron spectrometer (XPS), a quadrupole mass spectrometer (QMS) for temperature programmed desorption (TPD), and a Fourier transform infrared spectrometer (FTIR) for reflection–absorption infrared spectroscopy (RAIRS). The XPS system consists of a VG CLAM2 hemispherical analyzer and a dual anode X-ray source. Mg Kα radiation was used, and the spectrometer was calibrated with the Pt $4f_{7/2}$ peak at a binding energy of 71.2 eV. All RAIRS and TPD experiments were performed in a second chamber (chamber 2) with a base pressure of $\sim 2 \times 10^{-10}$ Torr. The system has been described in detail elsewhere.[29] In brief, this UHV chamber is equipped for LEED, Auger electron spectroscopy (AES), and TPD experiments with a QMS. The chamber is coupled to a commercial Fourier transform infrared spectrometer, a Bruker IFS 66 v/S. The IR beam enters and exits the UHV chamber through differentially pumped O-ring sealed KBr windows and passes through a polarizer before reaching the infrared detector. To achieve maximum sensitivity, an InSb detector was used with a tungsten source for the spectra obtained only in the region above 2000 cm^{-1}, while an MCT (HgCdTe) detector was used with a SiC source for the entire spectral range from 800 to 4000 cm^{-1}. A resolution of 4 cm^{-1} was used, except for the experimental results in Figure 8, which were obtained at a resolution of 2 cm^{-1}. In cases where the crystal was annealed above 85 K, it was cooled back down to 85 K before acquiring the spectra. All background spectra were also acquired at 85 K. For the TPD results, signal from the QMS was recorded for each mass while heating the crystal at a rate of 2 K/sec.

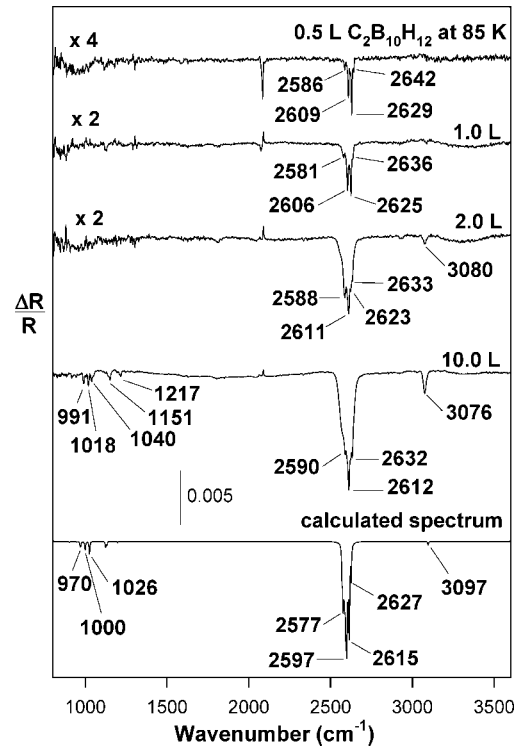

Figure 2. RAIR spectra of $C_2B_{10}H_{12}$ on Pt(111) as a function of exposure at 85 K. The spectrum at the bottom was calculated using DFT assuming a random orientation on the surface and Lorentzian line shapes with peak widths of 5 cm^{-1}. The calculated spectra represent a statistically weighted sum of spectra for the five most abundant isotopomers of carborane based on the natural abundance ratio of ^{10}B and ^{11}B.

The Pt(111) surfaces were cleaned and judged free of impurities by a standard procedure described earlier.[30] Briefly, the crystal was heated in $\sim 3 \times 10^{-7}$ Torr of O_2 at ~825 K for 1 h, after Ar^+ bombardment. Before exposing to carborane, the crystal was flashed to ~1200 K and cooled to 85 K. The carborane was purchased from Fisher Scientific with a quoted purity of 99%. It was further purified by transferring into a glass bulb and subjecting it to several freeze–pump–thaw cycles using a dry ice−acetone bath. The carborane was then condensed into another glass bulb cooled by liquid nitrogen. Finally, it was shielded from light to avoid any light-induced decomposition. For the RAIRS experiments, the Pt(111) surface was exposed to 2 L (Langmuir, 1 L = 1×10^{-6} Torr s) of carborane at 85 K. Then the surface was annealed to the designated temperatures, held for 30 s, and cooled down to 85 K before recording the spectra. All RAIR spectra have been baseline corrected.

Computational Method. The density functional theory (DFT) calculations were performed with the Gaussian 03 program package using the B3LYP (three-parameter hybrid Becke exchange and Lee–Yang–Parr correlation) functional. The triple-ζ plus polarization function 6–311G(d,p) basis set consisting of a polarization "d" function on B and C and a polarization "p" function on H was used. The structure of carborane was optimized first, and then vibrational frequencies were calculated for the optimized structure.

Results

Figure 2 shows the RAIR spectra of $C_2B_{10}H_{12}$ on Pt(111) as a function of increasing exposure with the surface at 85 K. At the lowest exposure of 0.5 L, only peaks in the B−H stretch region are visible, as these are by far the most intense

fundamentals of carborane. The weak feature just above 2000 cm^{-1} is due to CO adsorbed from the background, which is gradually displaced from the surface as the carborane coverage increases. The B−H stretch peaks undergo only modest changes in position and width with increasing exposure. For 0.5 L, four peaks are clearly resolved at 2586, 2609, 2629, and 2642 cm^{-1}. These peaks undergo small red shifts and changes in relative intensity with the 1.0 L exposure and are less well-resolved. Further broadening occurs in the 2.0 L spectrum, and the second lowest frequency peak is now at 2611 cm^{-1} and is the most intense. Also, a C−H stretch peak at 3080 cm^{-1} is visible in the 2.0 L spectrum. The 10.0 L spectrum corresponds to a multilayer of $C_2B_{10}H_{12}$ and features a similar B−H stretch intensity pattern as seen in the 2.0 L case, but now only three distinct B−H stretch peaks can be resolved at 2590, 2612, and 2632 cm^{-1}. The C−H stretch is readily apparent at 3076 cm^{-1}, and several weak peaks due to deformation modes are seen at 991, 1018, 1040, 1151, and 1217 cm^{-1}.

Also shown in Figure 2 is a simulated spectrum obtained from a DFT calculation of the isolated molecule. The frequencies in this spectrum were scaled by a factor of 0.9613, as recommended for the B3LYP hybrid functional and the 6–311G(d,p) basis set.[31] The intensities were calculated assuming a random orientation for the molecules on the surface. A Lorentzian lineshape function with a fwhm of 5 cm^{-1} was assumed for each peak in order to roughly match the experimental widths for the sharpest peaks. The simulation provides a good overall match for the 10 L spectrum indicating that the multilayer consists of randomly oriented undissociated carborane molecules. The simulation also reproduces the fact that B−H stretch vibrations are far more intense than any of the other modes. Thus, only the B−H stretch region and, to a much lesser extent, the C−H stretch region are likely to yield information on the bonding and reactions of $C_2B_{10}H_{12}$ on Pt(111). Since the B−H stretch frequencies for the multilayer are so similar to their values at the lowest exposures, we can conclude that the molecule adsorbs without dissociation at 85 K.

Figure 3 shows RAIR spectra in the B−H and C−H region as a function of annealing temperature following a 2.0 L exposure of $C_2B_{10}H_{12}$ to the Pt(111) surface at 85 K. The crystal was held at each temperature above 85 K for 30 s and then cooled back down to 85 K before acquiring the spectrum. The slight differences between the 85 K spectra in Figure 2 and those in Figure 3 reflect the degree of reproducibility of the exposures. The 200 K anneal produces sharper and therefore slightly more intense B−H stretch peaks, but their positions are largely unchanged as is the total peak area, which indicates that the molecule remains undissociated up to this temperature. The 200 K anneal also results in a sharper and more symmetric C−H stretch peak. The first sign of dissociation is observed at 250 K, where a new B−H stretch peak at 2499 cm^{-1} first appears. Because it is significantly different in frequency from the B−H stretches of the parent carborane, this peak is assumed to belong to a stable surface intermediate that retains B−H bonds. The 250 K spectrum is still dominated by the B−H stretches of carborane, with the 2604 cm^{-1} component now the most intense. The C−H stretch is also still visible in this spectrum and at 300 K, whereas by 350 K, there is only a trace of a B−H stretch peak of carborane. The B−H stretch of the new species has about the same intensity at 300 and 350 K; although in the former case, it consists of a main component at 2499 cm^{-1} with a shoulder at 2513 cm^{-1}, and in the 350 K spectrum, the peak is slightly broader and has shifted to 2507 cm^{-1}. For annealing temperatures of 400 K and above, the spectra are featureless,

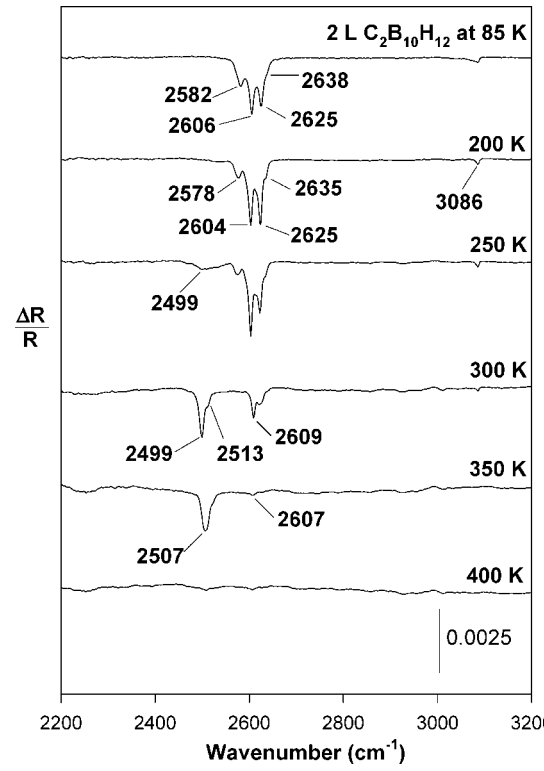

Figure 3. RAIR spectra following a 2 L $C_2B_{10}H_{12}$ exposure to the Pt(111) surface at 85 K and annealing to the indicated temperatures, after which the surface was cooled back to 85 K where the spectra were obtained.

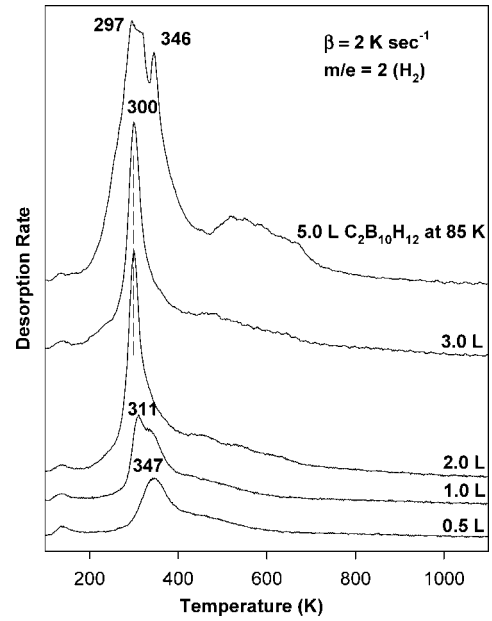

Figure 4. Temperature programmed desorption (TPD) results for H_2 as a function of $C_2B_{10}H_{12}$ exposure to Pt(111) at 85 K. The crystal was cleaned after each exposure.

suggesting either that all B−H and C−H bonds have dissociated or that surface species have been formed with B−H and/or C−H stretch vibrations that are simply too weak to be observed.

The dehydrogenation chemistry of carborane was also investigated with temperature programmed desorption (TPD). Figure 4 shows desorption of H_2 ($m/e = 2$) for a series of carborane exposures. At the lowest exposure, H_2 desorption is seen at about the same temperature as where hydrogen desorbs from the clean surface, which indicates that peaks in this

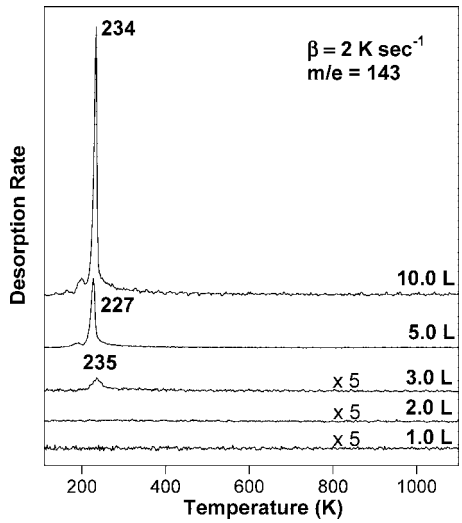

Figure 5. TPD spectra of $C_2B_{10}H_{12}$ as a function of $C_2B_{10}H_{12}$ exposure to the Pt(111) surface at 85 K. The most intense peak of the parent molecule occurs at a *m/e* value of 143, and this value was monitored with the mass spectrometer.

temperature range are desorption limited and that loss of hydrogen from carborane occurs at or below this temperature. For the 0.5 L exposure, there is presumably also a large contribution from H_2 that adsorbed from the background, but the growth of the peak at ~300 K with carborane exposure confirms that for the 1.0, 2.0, and 3.0 L cases dehydrogenation of the carborane occurs at or below ~300 K. The 5.0 L exposure shows a more complex peak shape in the ~300–350 K range, with a main peak at 300 K and a resolved component at 346 K. In all of the H_2 TPD traces in Figure 4, desorption is seen from 400 to 750 K, although only for the 5.0 L case is a distinct but broad peak observed. The retention of H on the surface to such high temperatures indicates that B−H and/or C−H bonds remain that do not give rise to B−H or C−H peaks observable with RAIRS. The TPD results for the parent molecule shown in Figure 5 show that the onset of multilayer formation occurs for carborane exposures somewhere between 3 and 5 L. For desorption of $C_2B_{10}H_{12}$, *m/e* = 143 was monitored as this is the most intense peak in the carborane mass spectrum. The peak shift from 227 to 234 K seen in Figure 5 as the exposure was increased from 5.0 to 10.0 L along with the strong increase in signal is indicative of the zero-order desorption expected for a multilayer. The absence of any desorption of the parent molecule for the 1.0 and 2.0 L exposures (and for 0.5 L, not shown) is consistent with complete dissociation of the molecule for submonolayer coverages. The desorption of carborane seen for the 3.0 L case at around 235 K in Figure 5 is probably indicative of desorption from the monolayer, suggesting that complete dissociation requires some empty sites.

Further information on the decomposition of carborane on Pt(111) is provided by X-ray photoelectron spectroscopy (XPS). Figure 6 shows the B 1s region following a 10.0 L exposure at 98 K and after annealing to 500, 600, and 700 K. In a separate experiment, the sample was annealed to 300 and 400 K following a 10 L exposure at 98 K. Each spectrum is the average of 60 scans using a pass energy of 20 eV and a step size of 0.4 eV. A 10.0 L exposure at 98 K results in a multilayer of carborane, as indicated by the TPD results, and corresponds to a narrow (fwhm = 2.0 eV) and symmetric B 1s peak at 190.6 eV. Annealing to higher temperatures results in a steady decrease of the intensity of the peak but no change in its shape or position. A plot comparing the B 1s peak area from XPS and the total

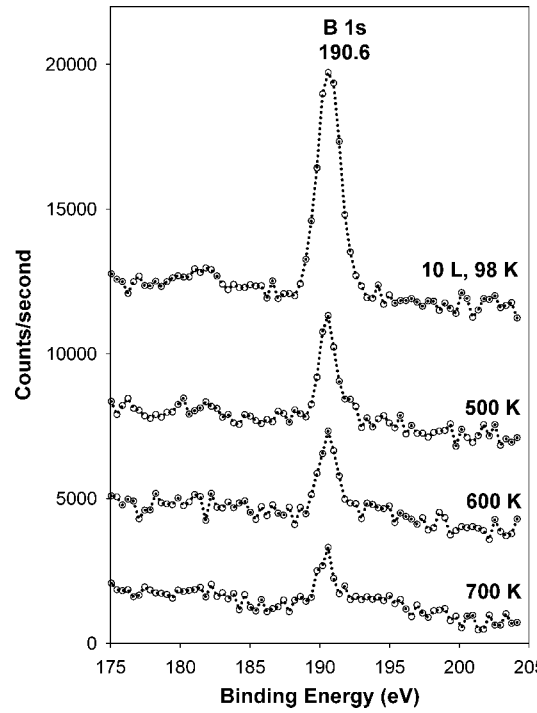

Figure 6. X-ray photoelectron spectra of the B 1s region following a 10 L exposure of $C_2B_{10}H_{12}$ to the Pt(111) surface at 85 K as a function of annealing temperature. Following each anneal, the crystal was cooled back to 85 K where the spectra were obtained. Each spectrum represents an average of 60 scans at a step size of 0.4 eV and a pass energy of 20 eV.

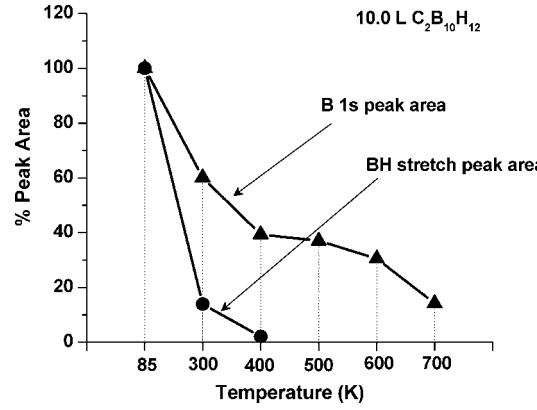

Figure 7. Comparison of the total BH stretch peak areas from RAIRS and the B 1s peak areas from XPS as a function of annealing temperature following a 10 L exposure of $C_2B_{10}H_{12}$ to the Pt(111) surface at 85 K.

peak area of the B−H stretch vibrations from RAIRS as a function of annealing temperature is shown in Figure 7. The comparison clearly reveals that boron remains on the surface to annealing temperatures well above the point where B−H stretch vibrations are no longer observable with RAIRS. The B 1s peak area decreases by 40% for the 300 K anneal corresponding to desorption of the multilayer. However, the TPD results indicate that carborane desorption should be complete by 400 K; yet, a 400 K anneal led to a further decrease in the B 1s signal. For higher annealing temperatures, there is a steady decrease in B 1s intensity, implying that boron is removed from the surface. Since B itself is nonvolatile in this temperature range, there are three possible ways to account for the decrease in B 1s signal. First, there may be desorption of a boron-containing species other than carborane. Any such species should

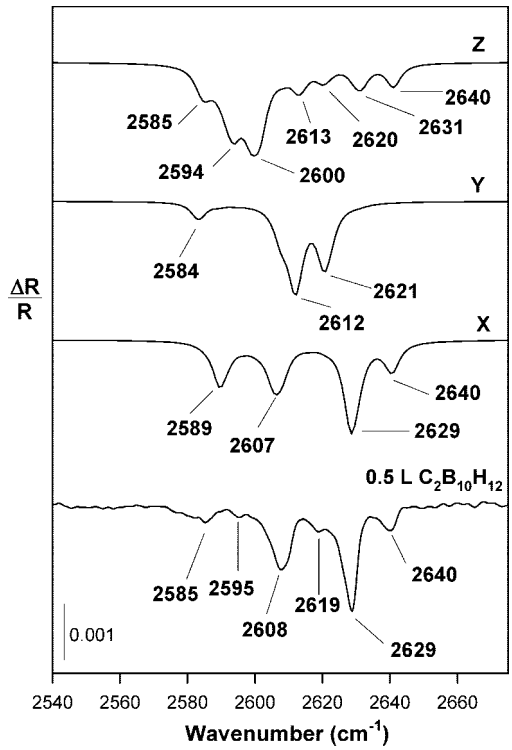

Figure 8. Comparison of experimental spectra of carborane on Pt(111) in the B−H stretch region with calculated spectra using DFT for an isolated molecule for the cases where the molecule's *x*, *y*, or *z* axes were oriented along the surface normal. The calculated spectra were scaled by a factor of 0.966 in order to align the highest frequency calculated B−H stretch with the experimental peak at 2640 cm^{-1}. The intensities of the calculated spectra were scaled such that the most intense calculated peak matched the intensity of the peak at 2629 cm^{-1}. A fwhm of 5 cm^{-1} was assumed for the calculated spectra. The experimental spectrum was obtained at a resolution of 2 cm^{-1} following a 0.5 L exposure to the crystal at 85 K. The calculated spectra represent a statistically weighted sum of spectra for the five most abundant isotopomers of carborane based on the natural abundance ratio of ^{10}B and ^{11}B.

presumably give a signal at $m/e = 11$ due to B atoms, but none was detected except for the fragment corresponding to the low temperature desorption of the parent carborane. Second, there may be some X-ray induced desorption of carborane or of its decomposition product. However, control experiments were performed that showed no decrease in B 1s area with time at a constant temperature under X-ray exposure, thus ruling out any photo- or photoelectron-induced desorption processes. Third, the molecule may fragment into boron atoms that diffuse into the bulk of the crystal, thus removing boron from the surface. Such a process should occur more readily at higher temperatures and likely accounts for the strong decrease between the 600 and the 700 K anneals. Some fragmentation may occur even at 400 K, which would explain the decrease seen for surface boron even at such a relatively low temperature.

Discussion

The experimental data presented can be analyzed to reach several conclusions regarding the adsorption and decomposition of carborane on Pt(111). The good agreement between the experimental spectra at submonolayer and multilayer coverages and the calculated spectra seen in Figure 2 indicates that at low temperatures the molecule adsorbs without dissociation and is not strongly perturbed through interactions with the surface. Comparisons between the calculated and the experimental spectra in the B−H stretch region can thus be used to infer the bonding geometry of the initially adsorbed molecule. Likewise, the changes seen with annealing temperature in the B−H stretch region can be used to infer the characteristics of the stable intermediate that forms through comparisons with known compounds containing B−H bonds. Ideally, conclusions reached with RAIRS can be correlated with the information obtained from TPD regarding the stages of hydrogen loss and from XPS regarding the fate of boron remaining on the surface after the RAIRS spectra become featureless.

A remarkable feature of the RAIRS results is the sharpness of the B−H stretch vibrations at low coverages at 85 K. For the 0.5 L $C_2B_{10}H_{12}$ exposure at 85 K shown in Figure 2, the measured fwhm of the 2629 cm^{-1} peak is only 5.6 cm^{-1}. Since the experimental resolution was 4 cm^{-1}, this implies that the intrinsic fwhm was less than 5 cm^{-1}, as confirmed in a separate experiment at 2 cm^{-1} resolution (Figure 8). This is in marked contrast with the experimental IR spectra of solid carborane where the B−H stretch appears as an intense band centered at ~2620 cm^{-1} with a fwhm of ~100 cm^{-1}, and under these circumstances, it is not surprising that there is no discernible difference in the B−H stretch band of the *ortho*, *meta*, and *para* isomers of solid carborane.[26] Our ability to resolve individual B−H stretch peaks makes it feasible to perform a detailed symmetry analysis as well as to consider the influence of the ^{10}B and ^{11}B natural isotopic distribution on the spectra. Because there are no suitable experimental reference spectra, we make use of the theoretical spectra from DFT calculations for this analysis. We base the analysis on the assumption that at low temperature the molecule is not strongly perturbed by interaction with the surface so that calculated spectra for an isolated, but oriented, molecule are appropriate.

The 10 B−H stretches of carborane can be assigned to the irreducible representations of the C_{2v} point group as follows:

$$\Gamma_{B-H} = 4A_1 + A_2 + 2B_1 + 3B_2$$

Since the A_2 mode is not IR active, only nine IR active B−H stretch fundamentals are expected. For C_{2v} symmetry, the dynamic dipole moments of the A_1 modes are oriented along the *z* axis as defined in Figure 1, while for the B_2 and B_1 modes, they are oriented along the *y* and *x* axes, respectively. If the adsorbed molecule retains C_{2v} symmetry, which is strictly possible only if the 2-fold rotation axis is aligned with the surface normal, then only the A_1 modes would be allowed by the surface dipole selection rule.[32] If, on the other hand, the molecules were randomly oriented on the surface, then all IR active modes of the isolated molecule would be allowed. Of course, for orientations in which the 2-fold axis is not perpendicular to the surface, the presence of the surface reduces the symmetry to at most the C_s point group. In this case, certain orientations would still retain a plane of symmetry and the A_1, B_1, and B_2 representations of the C_{2v} point group would correlate with the A′ (surface dipole allowed) and A″ (surface dipole forbidden) modes. If the adsorbed molecule were reduced to C_1, then even the A_2 modes of C_{2v} would become allowed. However, if the interaction with the surface is weak, then modes that would be allowed for C_s or C_1 symmetry but forbidden for C_{2v} should still be very weak as their dynamic dipole moments should still be roughly parallel to the surface. For example, if the 2-fold rotation axis (the *z* axis of the molecule) were parallel to the surface, with the *x* or *y* axes of the molecule along the surface normal, then either the B_1 or the B_2 modes of the C_{2v} point group would become surface dipole allowed. We therefore consider four hypothetical orientations: (1) a random orientation

in which the A_1, B_1, and B_2 modes are all allowed, (2) an orientation with the 2-fold rotation axis (z) aligned with the surface normal in which case only the A_1 modes are allowed, (3) an orientation with the molecule's x axis along the surface normal, in which only the B_1 modes should have appreciable intensity, and (4) an orientation with the molecule's y axis along the surface normal, in which only the B_2 modes should have appreciable intensity. Again, strictly speaking, for cases 3 and 4, the molecule on the surface can have at most C_s symmetry in which both A_1 and B_1 of C_{2v} (A′ of C_s; orientation 3) or A_1 and B_2 (orientation 4) would be formally allowed. However, the A_1 modes in these two cases are unlikely to have appreciable intensity.

A complicating factor in the vibrational spectroscopy of boron compounds is the presence of ^{10}B and ^{11}B isotopes in a natural abundance ratio of 1:4. Since the harmonic frequency of the diatomic molecule ^{10}BH should be 10 cm^{-1} higher than for ^{11}BH and since our B−H stretches have widths less than half of this, we need to account for the frequencies of all isotopomers that might make a significant contribution to the measured spectra. It is a fairly straightforward process to include the various isotopomers in the DFT calculations and then to apply the correct statistical weighting in summing the intensities to calculate the theoretically predicted spectra for an isolated $C_2B_{10}H_{12}$ molecule with the natural abundance ^{11}B:^{10}B ratio. This shows, for example, that the B−H stretch frequencies of the all-^{10}B isotopomer of $C_2B_{10}H_{12}$ are 11–12 cm^{-1} higher than the corresponding frequencies for the all-^{11}B isotopomer. Although the all-^{10}B isotopomer has a negligible statistical weighting of only 9×10^{-8}, the five isotopomers of a B_{10} unit with the highest weightings are $^{11}B_8{}^{10}B_2$ (0.295), $^{11}B_9{}^{10}B_1$ (0.266),$^{11}B_7{}^{10}B_3$ (0.194), and $^{11}B_{10}$ (0.108), and $^{11}B_6{}^{10}B_4$ (0.0839). All possible isotopic distributions that lead to different vibrational spectra were taken into account for these five most important isotopomers. For example, in the $^{11}B_8{}^{10}B_2$ isotopomer, vibrational spectra were calculated for all nonequivalent structures arising from placing the two ^{10}B atoms on different boron sites of the molecule. Then, all of these spectra were summed, and the corresponding statistical weighting factor was applied. The calculations definitely predict measurable effects on the spectra, in contrast to the statement in ref 26 that, in the case of the $B_{12}H_{12}{}^{2-}$ ion, the separation between isotopomers is not more than 1 cm^{-1} and can therefore be ignored. Similarly, Salam et al. state that splittings in the B−H stretch region of carborane less than 10 cm^{-1} would be too small to be observed.[27] Thus, the sharpness of the B−H stretch vibrations observed here is contrary to general expectations and demonstrates the opportunity for more detailed vibrational analysis of the RAIR spectra of boranes and carboranes on surfaces than is warranted in more conventional spectroscopic studies of these compounds.

Figure 8 shows a comparison of the experimental B−H stretch region obtained after a 0.5 L exposure at 85 K with calculated spectra for three assumed orientations. The calculated spectra contain statistically weighted contributions from the five most important isotopomers. The experimental spectrum was obtained with a resolution of 2 cm^{-1} to yield a measured fwhm of 4.8 cm^{-1} for the 2629 cm^{-1} peak, implying that the intrinsic fwhm of the peak is 4.4 cm^{-1}. The other peaks are slightly broader. An assumed fwhm of 5 cm^{-1} was used for the calculated spectra. The calculated frequencies were scaled by a factor of 0.966 in order to bring the highest calculated B−H stretch frequency into alignment with the experimental frequency at 2640 cm^{-1}. This scale factor is only slightly larger than the standard value of 0.961 for a DFT calculation with this basis set. It is also quite close to a recently recommended value of 0.9669 ± 0.0205 for a B3LYP calculation with the 6–311G(d,p) basis set.[33] The intensities of the calculated spectra were scaled so that the most intense calculated peak matched the intensity of the 2629 cm^{-1} peak of the experimental spectrum. Spectra are calculated for the x, y, or z axes of the molecule oriented along the surface normal.

The first conclusion that can be reached from Figure 8 is that the molecule is not randomly oriented on the surface. Such a case would give a spectrum that is simply the addition of the three spectra for x, y, and z orientations, which would clearly result in a much more complicated spectrum than observed. Of the three orientations, the spectrum labeled x gives much better agreement with the experimental spectrum than do the y and z spectra. The x spectrum shows a good match in frequency and relative intensity with the experimental spectrum for the peaks at 2640, 2629, and 2608 cm^{-1} but a less satisfactory match with the lowest frequency peak at 2585 cm^{-1}. Also the weak peaks in the experimental spectrum at 2619 and 2595 are not present in the x spectrum. This may indicate that the orientational order is not perfect, with some y and z oriented molecules also present.

A plausible explanation for the orientation with the molecule's x axis perpendicular to the surface is that the dipole moment would then be parallel to the surface, which would give the most favorable interaction with its image dipole. With this orientation, the dipole–dipole interaction among the adsorbed molecules could also be minimized. Since *ortho*-carborane has a substantial permanent dipole moment of 4.49 Debye,[27] it is not surprising that the molecule adopts a preferred orientation on the surface. With the x axis along the surface normal, the C−C bond is oriented parallel to the surface, which might allow both carbon atoms, which have a large positive charge, to interact with the Pt atoms, which would not be the case with the y axis along the surface normal. This reasoning would suggest that the 1,12 isomer (*para*-carborane), which has no permanent dipole moment, would adopt a random orientation on the Pt(111) surface. Interestingly, primarily on the basis of ultraviolet photoemission results, Zeng et al. also proposed that *ortho*-carborane interacts with the Cu(100) surface through the carbon atoms.[23] In a study using photoemission and inverse photoemission spectroscopies to compare the electronic structure of *ortho*-, *meta*-, and *para*-carborane adsorbed on a variety of substrates, Balaz et al. found a clear correlation between the magnitude of the dipole moment and the position of the adsorbate energy levels relative to the Fermi level.[34] Thus, both their study and our study indicate that the molecular dipole moment plays a dominant role in the electronic and geometric structures of these three isomeric *closo*-carboranes on metal surfaces.

The B−H stretch of the intermediate formed by annealing the carborane-covered surface to 300 K consists of a main component at 2499 and a shoulder at 2513 cm^{-1}. The fact that these frequencies are substantially red-shifted from the parent carborane clearly indicates the formation of a distinctly different chemical species. In Leites' survey of the vibrational spectroscopy of carboranes and boranes, the B−H stretch of a series of five *closo*-carboranes show little variation from a low value of 2600 cm^{-1} for 1,10-$C_2B_8H_{10}$ to a high value of 2660 cm^{-1} for 1,5-$C_2B_4H_6$. In contrast, the corresponding *closo*-borane anions are centered below 2500 cm^{-1}. Brint et al.[35] have specifically considered the correlation of B−H stretching frequencies with bonding for both neutral boranes as well as borane anions. For the neutral molecules, they found typical B−H stretch values of 2368, 2497, and 2763 cm^{-1} for hybridization at the boron

atom of sp^3, sp^2, and sp, respectively. For *closo* borane anions of the form $B_nH_n^{2-}$ with $n = 6$, 8, 9, 10, 11, and 12, they found that the B−H stretch frequencies fell in a narrow range of 2440–2540 cm^{-1}. The clear implication from the B−H stretch frequency of our surface intermediate is that it is a $B_nH_n^{2-}$ anion. The simplest hypothesis is that, since the C−H stretch peak vanishes as carborane is converted to the intermediate, the CH groups are removed to form $B_{10}H_{10}^{2-}$, a well-known and stable anion with a B−H stretch at 2471 cm^{-1}.[26] At the other extreme in the fragmentation of carborane would be the formation of BH molecules on the surface. However, the fundamental of gas phase ^{11}BH is at 2268 cm^{-1}.[36] Although it is not known how much this would shift upon adsorption, a more than 200 cm^{-1} blue shift seems unlikely. A completely different possibility is the formation of dicarbollide ($C_2B_9H_{11}^{2-}$) anions, which are well-known to form complexes with metals. The B−H stretch vibrations in a series of dicarbollide complexes with Ni, Pd, and Pt[37], had values in the range of 2520 to 2580 cm^{-1}, with the Pt complex having a value of 2564 cm^{-1}. Although these values are a bit higher than observed for our intermediate, the difference is not so large as to completely rule out this possibility. The best strategy for making a more definitive identification of the intermediate is to calculate the stability and vibrational spectrum of possible species and to see which one provides the best match with the observed spectrum. Such calculations are currently underway.

There is a remarkable similarity in the icosahedral structures of the $C_2B_{10}H_{12}$ carboranes and the icosahedral structures found in boron carbide. Although the stoichiometry of boron carbide is often given as B_4C, Bouchacourt and Thevenot[38] reported that the homogeneity range for rhombohedral boron carbide ranges from 20 to 8.8% carbon, corresponding to stoichiometries of B_4C to $B_{10.4}C$. The most carbon rich compositions have structures consisting of $B_{11}C$ icosahedra and CBC chains along the rhombohedral 3-fold symmetry axis. As the carbon content is reduced, boron replaces carbon in the three-atom chains rather than in the icosahedra so that the $B_{11}C$ stoichiometry of the latter is preserved. According to this idea, a boron carbide produced from carborane would consist of a mixture of $B_{11}C$−CBC and $B_{11}C$−BBC structures in order to obtain an overall B_5C stoichiometry. The similarity of the bonding within the $B_{10}C_2$ icosahedra of carborane and $B_{11}C$ of boron carbide (B_4C) is reflected in the B−B distances, which range from 1.756 to 1.810 Å in the latter[39] and from 1.745 to 1.810 Å in the former.[40] The fact that boron carbide thin films can be grown by chemical vapor deposition using carborane as a precursor might suggest icosahedral structures are preserved in the process. If so, the boron carbide structure would have to be initially formed from icosahedral units that still retained considerable hydrogen, as there is ample evidence in the literature that icosahedral structures are not favored for bare B_{12} or $B_{10}C_2$ clusters.

In a series of papers, Boustani and co-workers have used theoretical methods to determine the most stable structures formed by boron clusters of various sizes. Boustani finds that the three most stable isomers of B_{12} have two planar structures of C_{2v} and D_{2h} symmetry and a convex structure of C_{3v} symmetry.[41] Similarly, they found that B_{32} clusters formed quasiplanar or tubular structures.[42] They specifically studied a cluster consisting of 96 boron atoms to see if it would adopt the bonding arrangement of the eight B_{12} icosahedra at the corners of a unit cell of α-rhombohedral boron.[43] However, structures involving quasiplanar sheets or tubes were found to be more stable. Park et al.[44] calculated the optimized structure of a $B_{10}C_2$ cluster and found it to be similar to the quasiplanar structures found by Boustani with the carbon atoms on opposite edges. Park et al.[44] were specifically interested in the relationship between their calculated structures and structures that might be present in boron carbide thin films derived from carborane. They noted that the vibrations associated with the $B_{10}C_2$ icosahedra in carborane have frequencies less than 1200 cm^{-1}, whereas Raman spectra of the boron carbide grown from carborane shows Raman peaks at 1365 and 1600 cm^{-1}. Simulated Raman spectra for a mixture of the quasiplanar $B_{10}C_2$ showed reasonable agreement with the experimental spectra, providing some evidence that the films derived from carborane contained such structural units, rather than $B_{11}C$ icosahedra. However, other studies[45] of rhombohedral boron carbide show infrared bands at ~1600 cm^{-1}, which are attributed to asymmetric stretching of the CBC chains. For a boron carbide structure lacking a center of symmetry, it would be possible for this mode to be both Raman and IR active. Thus, the observation of such a high frequency Raman peak by Park et al.[44] does not necessarily rule out a boron carbide structure in their thin films of the usual type involving boron-rich icosahedra.

Conclusions

Ortho-carborane adsorbs molecularly at submonolayer coverages on the Pt(111) surface at 85 K as indicated by the similarity of its RAIR spectrum to both the infrared spectrum of the molecular solid and the IR spectrum calculated with DFT for the isolated molecule. The RAIR spectrum for the molecularly adsorbed molecule displays narrow B−H stretch peaks with fwhm as narrow as 4.4 cm^{-1}, as compared to widths of over 100 cm^{-1} reported in the literature for the molecular solid. The sharpness of the B−H stretch vibrations allows a detailed analysis of the spectrum in terms of molecular orientation and indicates that the molecule adsorbs with both the dipole moment and the C−C bond aligned parallel to the surface. The platinum surface promotes the thermal decomposition of the molecule below 300 K to produce a stable surface intermediate characterized by a B−H stretching vibration at 2507 cm^{-1}. A comparison with the B−H stretch frequencies of known compounds suggests that the intermediate is an anionic $B_nH_n^{2-}$ species. Heating to temperatures of 400 K and above results in a featureless RAIR spectrum, but TPD shows hydrogen desorption up to 700 K, indicating that hydrogen-containing surface intermediates are present to high temperatures. Boron is lost from the surface upon heating to 700 K as indicated by XPS, presumably because of dissolution of boron into the bulk of the platinum crystal.

Acknowledgment. This work is supported by the Department of Energy under Grant DE-FG02-05ER15726 and by the National Science Foundation under Grant CHE-0714562. D.S. acknowledges the financial support of the Department of Defense and the National Science Foundation under Grant NSF EEC 0453432.

References and Notes

(1) Cotton, F. A.; Wilkinson, G. *Advanced Inorganic Chemistry: A Comprehensive Text*, 4th ed.; Wiley: New York, 1980.
(2) Davidson, G. *Coord. Chem. Rev.* **1983**, *49*, 117.
(3) Grimes, R. N. *Carboranes*; Academic Press: New York, 1970.
(4) Lipscomb, W. N. *Boron Hydrides*; W. A. Benjamin: New York, 1963.
(5) Muetterties, E. L. *Polyhedral boranes*; M. Dekker: New York, 1968.
(6) Muetterties, E. L. *Boron hydride chemistry*; Academic Press: New York, 1975.
(7) Greenwood, N. N. *Chemistry of the elements, 2nd ed.*; Greenwood, N. N., Earnshaw, A., Eds.;Butterworth-Heinemann Oxford: Boston, 1997.

(8) Crabtree, R. H. *The organometallic chemistry of the transition metals*; Wiley: New York, 1988.
(9) Evans, W. J.; Dunks, G. B.; Hawthorne, F. M. *J. Am. Chem. Soc.* **1973**, *95*, 4565.
(10) Gaines, D. F.; Steehler, G. A. *Chem. Commun.* **1982**, *2*, 122.
(11) Greenwood, N. N. *Chem. Soc. Rev.* **1974**, *3*, 231.
(12) Greenwood, N. N. *Pure Appl. Chem.* **1983**, *55*, 1415.
(13) Grimes, R. N. *Metal interactions with boron clusters*; Plenum Press: New York, 1982.
(14) Grimes, R. N. *Metallocarboranes and Metalloboranes*; Pergamon: Oxford, 1995; Vol. 1.
(15) Salentine, C. G.; Hawthorne, F. M. *Inorg. Chem.* **1976**, *15*, 2872.
(16) Balaz, S.; Dimov, D. I.; Boag, N. M.; Nelson, K.; Montag, B.; Brand, J. I.; Dowben, P. A. *Appl. Phys. A: Mater. Sci. Process.* **2006**, *84*, 149.
(17) Byun, D.; Hwang, S.-d.; Zhang, J.; Zeng, H.; Perkins, F. K.; Vidali, G.; Dowben, P. A. *Jpn. J. Appl. Phys* **1995**, *34*, L941.
(18) Caruso, A. N.; Balaz, S.; Xu, B.; Dowben, P. A.; McMullen-Gunn, A. S.; Brand, J. I.; Losovyj, Y. B.; McIlroy, D. N. *Appl. Phys. Lett.* **2004**, *84*, 1302.
(19) Caruso, A. N.; Dowben, P. A.; Balkir, S.; Schemm, N.; Osberg, K.; Fairchild, R. W.; Flores, O. B.; Balaz, S.; Harken, A. D.; Robertson, B. W.; Brand, J. I. *Mater. Sci. Eng. B* **2006**, *135*, 129.
(20) Lunca-Popa, P.; Brand, J. I.; Balaz, S.; Rosa, L. G.; Boag, N. M.; Bai, M.; Robertson, B. W.; Dowben, P. A. *J. Phys. D: Appl. Phys.* **2005**, *38*, 1248.
(21) Bernard, L.; Caruso, A. N.; Xu, B.; Doudin, B.; Dowben, P. A. *Thin Solid Films* **2003**, *428*, 253.
(22) Caruso, A. N.; Bernard, L.; Xu, B.; Dowben, P. A. *J. Phys. Chem. B* **2003**, *107*, 9620.
(23) Zeng, H.; Byun, D.; Zhang, J.; Vidali, G.; Onellion, M.; Dowben, P. A. *Surf. Sci.* **1994**, *313*, 239.
(24) Zhang, J.; McIlroy, D. N.; Dowben, P. A.; Zeng, H.; Vidali, G.; Heskett, D.; Onellion, M. *J. Phys. Condens. Matter* **1995**, *7*, 7185.
(25) Orimo, S. i.; Nakamori, Y.; Eliseo, J. R.; Zuttel, A.; Jensen, C. M. *Chem. Rev.* **2007**, *107*, 4111.
(26) Leites, L. A. *Chem. Rev.* **1992**, *92*, 279.
(27) Salam, A.; Deleuze, M. S.; Francois, J. P. *Chem. Phys.* **2003**, *286*, 45.
(28) Kang, D. H.; Trenary, M. *Surf. Sci.* **2000**, *470*, L13.
(29) Brubaker, M. E.; Trenary, M. *J. Chem. Phys.* **1986**, *85*, 6100.
(30) Jentz, D.; Celio, H.; Mills, P.; Trenary, M. *Surf. Sci.* **1995**, *341*, 1.
(31) Foresman, J. B.; Frisch, A. *Exploring Chemistry with Electronic Structure Methods*; Gaussian Inc.: Pittsburgh, 1996.
(32) Fan, J.; Trenary, M. *Langmuir* **1994**, *10*, 3649.
(33) Irikura, K. K.; Johnson, R. D.; Kacker, R. N. *J. Phys. Chem. A* **2005**, *109*, 8430.
(34) Balaz, S.; Caruso, A. N.; Platt, N. P.; Dimov, D. I.; Boag, N. M.; Brand, J. I.; Losovyj, Y.; Dowben, P. A. *J. Phys. Chem. B* **2007**, *111*, 7009.
(35) Brint, P.; Sangchakr, B.; Fowler, P. W.; Weldon, V. J. *J. Chem. Soc., Dalton Trans.* **1989**, 2253.
(36) Huber, K. P.; Herzberg, G. *Constants of Diatomic Molecules*; Van Nostrand Reinhold Company: New York, 1979.
(37) Warren, L. F.; Hawthorne, M. F. *J. Am. Chem. Soc.* **1970**, *92*, 1157.
(38) Bouchacourt, M.; Thevenot, F. *J. Less-Common Met.* **1981**, *82*, 219.
(39) Kwei, G. H.; Morosin, B. *J. Phys. Chem.* **1996**, *100*, 8031.
(40) Bohn, R. K.; Bohn, M. D. *Inorg. Chem.* **1971**, *10*, 350.
(41) Boustani, I. *Phys. Rev. B* **1997**, *55*, 16426.
(42) Boustani, I.; Rubio, A.; Alonso, J. A. *Chem. Phys. Lett.* **1999**, *311*, 21.
(43) Boustani, I.; Quandt, A.; Rubio, A. *J. Solid State Chem.* **2000**, *154*, 269.
(44) Park, K.; Pederson, M. R.; Boyer, L. L.; Mei, W. N.; Sabirianov, R. F.; Zeng, X. C.; Bulusu, S.; Curran, S.; Dewald, J.; Day, E.; Adenwalla, S.; Diaz, M.; Rosa, L. G.; Balaz, S.; Dowben, P. A. *Phys. Rev. B* **2006**, *73*.
(45) Lazzari, R.; Vast, N.; Besson, J. M.; Baroni, S.; Dal Corso, A. *Phys. Rev. Lett.* **1999**, *83*, 3230.

JP8011975